Design and construction of system for sub - 20fs pulses through self-phase modulation.

A Thesis Presented

by

Richard Jason Brown

to

The Graduate School

in Partial Fulfillment of the Requirements

for the Degree of

Master of Science

in

Physics

Scientific Instrumentation

Stony Brook University

May 2006

Stony Brook University

The Graduate School

Richard Jason Brown

We, the Thesis committee for the above candidate for the Master of Science degree, hereby recommend acceptance of the Thesis.

Thomas C. Weinacht, Thesis Advisor

Assistant Professor, Department of Physics and Astronomy, Stony Brook University

---

Deane Peterson

Professor, Department of Physics and Astronomy, Stony Brook University

---

James Lukens

Professor, Department of Physics and Astronomy, Stony Brook University

---

Michael Rijjsenbeek

Professor, Department of Physics and Astronomy, Stony Brook University

This Thesis is accepted by the Graduate School.

Dean of the Graduate School

Abstract of the Thesis

Design and construction of system for sub - 20fs pulses through self-phase modulation.

by

Richard Jason Brown

Master of Science

in

Physics

Scientific Instrumentation

Stony Brook University

2006

In this thesis we present a the design and construction of an inexpensive, efficient, and easily built system to produce sub-20fs pulses with broad bandwidth and good spatial mode. A vacuum cell filled with a noble gas (Argon) was used to create the medium in which the pulses would interact. Through the use of a nonlinear optical technique known as self phase modulation (SPM) we were able to obtain a pulse duration $\tau = 19$ fs, with a good spatial mode spot size of 1.6 mm, consistently with an efficiency of 93%. The pulses were characterized using FROG. τ was measured as a function of argon gas pres-

sures and pulse energies to find the best combination of both that would yield the shortest pulse. Results will be further discussed.

Contents

List of Figures

List of Tables

Acknowledgements

Write your acknowledgements here...

Chapter 1

Introduction

Stable, mode-locked,and broad bandwidth ultrafast lasers were a revolutionary introduction in the early 1990's [1]. Since then, ultrafast lasers have been used in medical fields [2], ultrafast spectroscopy of semiconductors [3], control of spectral polarization [4], coherent control [5, 6], Femtochemistry [7, 8],atomic physics [9], and strong electric field atomic physics [10].

The term ultrafast is generally used to refer to laser pulses of subpicoseond duration. Commercially available Kerr Lens modelocked titanium sapphire lasers (an oscillator) are capable of producing pulses with time durations, τ, of about 20fs. This meets our demands for pulse duration, but not for peak pulse power. THe oscillator can produce pulses with energies of about $4nJ$ from an averge intensity of 400 mW and a rep rate of about 100 MHz. The amplifier is used to amplify the pulse energies. The consequence fom using the

amplifier is gain narrowing [11]. As the pulse passes through the amplifier there is a loss in spectral bandwidth and a temporal broadening of τ in time. Pulses with durations of about 30-35fs and energies of $900\mu J$-$1mJ$ at a wavelength $\lambda = 780$ nm are typical for our amplified system. These pulse have a rep rate of about 1 kHz. We need amplified pulses because in our lab we strong field atomic and molecular physics. If one focuses a 30fs pulse with 1mJ of energy to a spot size of 10μm, fields on the order of $10^{11}v/m$ are easily acquired.

The goal of the thesis was to produce an inexpensive, and efficient system to create sub-20fs pulses and maintain the high pulse energies obtained from the amplifier. This can be accomplished by using nonlinear optical techniques, such as self-phase modulation (SPM),detailed in chapter 2, to broaden the spectral bandwidth after amplification. If the spectral phase of the extended bandwidth can be controlled, then one can generate pulses with durations significantly shorter than the pulses directly exiting the amplifier system. Since we are adding bandwidth to the pulse from SPM, the broadening effect from dispersive material is amplified. Controlling the phase and compressing the pulse can be done with chirped mirrors, which are further discussed in chapter 2.

There have been others in the ultrafast field to create this type of system and have had high success[12, 13]. This one group in particular, Ursula Keller's

group, has been able to obtain pulses as short as 5-7fs through the use of SPM in a hollow core fiber. While making use of SPM in a hollow core fiber has been demonstrated to yield pulses as short as 5-7 fs, the efficiency is typically below 50%, the construction and alignment of the fiber everyday is tedious and the materials are relatively expensive. We sought an alternative that would be more efficient, easy to align and inexpensive. This thesis describes the design construction and testing of an apparatus for producing sub 20 fs amplified laser pulses through filamentation based self phase modulation in an argon cell followed by pulse compression using chirped ultrafast laser mirrors

We will move through a basic discussion on the background of the device in chapter 2, the design and construction of the device in chapter 3, and measurements and results in chapter 4.

Chapter 2

Basic principles

This chapter will cover the basic principles involved. It will present three main topics: a brief discussion on Gaussian beams, nonlinear effects of self-phase modulation, and what is Group Velocity Dispersion (GVD) and how do we compensate?.

2.1 A brief discussion on Gaussian beams

This section will cover some basics on Gaussian beam propagation, and the calculation of the various parameters used to define Gaussian beams through the ABCD law.

2.1.1 Beam propagation

Here we will describe the propagation of the beam through my system using Gaussian beam formalism.

The basic Gaussian beam intensity profile for a laser beam has the form

$$I(x, y, z) \sim I_0 e^{-2(x^2+y^2)/w(z)^2} \tag{2.1}$$

$$I_0 = \frac{1}{2}\epsilon_0 c E_0^2, \tag{2.2}$$

where $w(z)$ is the spot size of the beam projected on a screen [14]. There are various methods used to specify $w(z)$, and must be explicitly stated when quoting a spot size. For this thesis $w(z)$ will be measured by the 1/e point of the gaussian beam for the electric field.

We should also consider that the spot size of a laser beam varies with the distance of propagation. Figure 2.1 shows the shape of the beam as it propagates a distance in z.

The parameter b is the confocal parameter which is exactly $2z_0$, where z_0 is the Rayleigh range. The Rayleigh range is defined as the point at which the spot size $w(z)$ of the beam has grown to $\sqrt{2}w_0$. The spot size at the beam waist is w_0. The divergence of the beam is given by

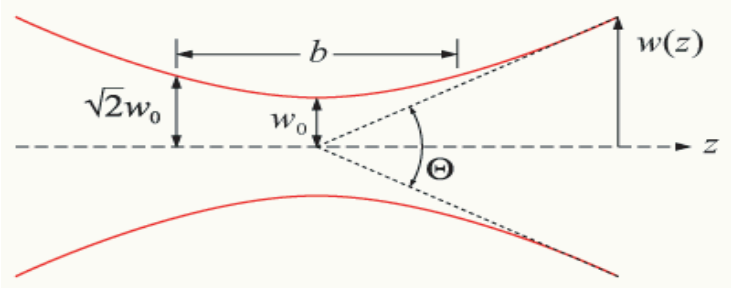

Figure 2.1 As a the beam propagates there is an intrinsic waist associated with it.

$$\theta = \frac{\lambda}{\pi w_0} \tag{2.3}$$

with

$$\Theta = 2\theta \tag{2.4}$$

and the Rayleigh range

$$z_0 = \frac{\pi w_0}{\lambda} \tag{2.5}$$

2.1.2 The matrix representation for Gaussian beams

The matrix formulae Gaussian beams allows us to monitor how the beam is transformed as it propagates through an optical system. Making use of the ray matrices used in geometrical optics we have, for our system, three main optical elements.

The beam first passes through a plano-convex lens into the cell. We can assume the window on the cell is not contributing to the transformation of

the pulse, but just adding phase. The beam then travels a length L through a medium, in this case argon gas, before bouncing off two curved mirrors positioned in such a way as to obtain a collimated beam.

After combining the ray matrices found in [14] we can calculate the ray matrix for our optical system, and it looks as follows.

$$\begin{pmatrix} A & B \\ C & D \end{pmatrix} = \begin{pmatrix} 1 & 0 \\ -\frac{2}{f_3} & 1 \end{pmatrix} \begin{pmatrix} 1 & L_1 \\ 0 & 1 \end{pmatrix} \begin{pmatrix} 1 & 0 \\ -\frac{2}{f_2} & 1 \end{pmatrix} \begin{pmatrix} 1 & L_2 \\ 0 & 1 \end{pmatrix} \begin{pmatrix} 1 & 0 \\ -\frac{1}{f_1} & 1 \end{pmatrix} \tag{2.6}$$

Using the q parameters for gaussian beams, we can relate to our ray matrix, a beam radius of curvature and a new spot size.

2.2 Non-Linear optics

2.2.1 Nonlinear Polarization

As a light travels through a transparent medium, the electric field field induces a polarization in that medium. This is the response due to electrons oscillating inside the medium. In a dielectric medium we have a linear polarizability

$$P = \epsilon_0 \chi E \tag{2.7}$$

where $\chi = \epsilon - 1$ is the electric susceptibility. Relationships for the displacement D, polarization P, and electric field E [15]can be written as

$$\begin{aligned} D = \epsilon\epsilon_0 E &= \epsilon_0 E + P \\ P &= \epsilon_0 \chi E \end{aligned} \tag{2.8}$$

If there exists a medium that elicits a nonlinear response one must take into account the higher order terms that can be found through a series expansion.

$$P = \epsilon_0[\chi^{(1)}E + \chi^{(2)}E^2 + \chi^{(3)}E^3 + \cdots] \tag{2.9}$$

$$= P^L + P^{NL} \tag{2.10}$$

where $\chi^{(1)}$ is the linear term, $\chi^{(2)}$ is responsible for second harmonic generation(SHG) in crystals without inversion symmetry. SHG provides the gating mechanism for our pulse measurement through Frequency Resolved Optical Gating (FROG). FROG will be briefly discussed in Chapter 4. The $\chi^{(3)}$ term is responsible for the optical (AC) Kerr effect, nonlinear index of refraction, self-phase modulation, and self-focussing.

2.2.2 Optical Kerr effect

The optical Kerr effect, also known as the AC Kerr effect, is where a highly intense beam can create its own modulating electric field. No external field is

applied. The electric field can be defined as

$$E = E_0(t)cos(\omega t) \tag{2.11}$$

where $E_0(t)$ is the slowly varying envelope amplitude of the electric field which does not vary substantially over one optical cycle. The equation above if for the temporal variations of the electric field. If we substitute 2.11 into 2.9 and ignore all terms except the linear and $\chi^{(3)}$ terms we get

$$\begin{aligned} P &= \epsilon_0[\chi^{(1)}\cos(\omega t) + \chi^{(3)}E_0^2(t)\cos^3(\omega t)]E_0(t) && (2.12)\\ &= \epsilon_0(\chi^{(1)}\cos(\omega t) + \frac{\chi^3}{4}E_0^2(t)[3\cos(\omega t) + \cos(3\omega t)])E_0(t) && (2.13) \end{aligned}$$

Equation 2.13 has a ωt term and a $3\omega t$(third-harmonic generation) term. Neglecting the 3ω term, because it is not of the interest of this thesis, and simplifying shows

$$P = \epsilon_0(\chi^{(1)} + \frac{3\chi^3}{4}E_0^2(t))E_0(t)\cos(\omega t)) \tag{2.14}$$

As done before for P, χ can be written as

$$\begin{aligned} \chi &= \chi^L + \chi^{NL} && (2.15)\\ &= (\chi^{(1)} + \frac{3}{4}\chi^{(3)}E_0(t)^2) && (2.16) \end{aligned}$$

The refractive index for a medium is defined as

$$\begin{aligned} n &= [1+\chi]^{(\frac{1}{2})} && (2.17)\\ &= \sqrt{(}\varepsilon) && (2.18) \end{aligned}$$

where from 2.8 above

$$\varepsilon = \varepsilon_L + \varepsilon_{NL} \tag{2.19}$$

$$= (1 + \chi^{(1)} + \frac{3}{4}\chi^{(3)}) \tag{2.20}$$

where ε is the dielectric permittivity, and

$$n = \sqrt{\varepsilon_L + \varepsilon_{NL}} \simeq \varepsilon_L(1 + \frac{\varepsilon_{NL}}{2\varepsilon_L}) \tag{2.21}$$

Now one can arrive at an intensity dependent index of refraction

$$n = n_0 + \frac{3\chi^{(3)}}{8n_0}|E_0(t)|^2 \tag{2.22}$$

$$= n_0 + n_2 I(t) \tag{2.23}$$

2.2.3 Self-phase modulation

If an ultrashort pulse of light travels through a medium, a time varying index of refraction of the medium from the optical Kerr effect induces a phase shift in the pulse. This leads to additions to the pulse's frequency spectrum. The details of this will be outlined below.

If the electric field in the time-domain is represented as

$$E(t) = E_0 \exp(\imath\varphi(t)) \tag{2.24}$$

then we can write the phase as

$$\varphi(t) = \omega_0 t - \beta z \tag{2.25}$$

where

$$\beta = \frac{n\omega_0}{c} \tag{2.26}$$

where ω_0 is the carrier frequency and c is the speed of light in a vacuum. Substituting for n yields

$$\begin{aligned} \varphi(t) &= \omega t - \frac{\omega_0}{c}[n_0 + n_2 I(t)]z & (2.27) \\ &= \omega t - k_0 z - \frac{n_2\omega_0}{c} z I(t) & (2.28) \end{aligned}$$

If we separate the linear terms and nonlinear terms, the nonlinear portion of the phase becomes

$$\varphi_{NL} = -\frac{n2\omega_0}{c} z I(t) \tag{2.29}$$

We define the instantaneous frequency as

$$\omega = \frac{d\varphi}{dt} = \omega_0 - \frac{n_2\omega_0}{c} z \frac{dI(t)}{dt} \tag{2.30}$$

where the second term in equation 2.30 is the frequency shift induced from the nonlinear index of refraction.

$$\delta\omega = -\frac{n_2\omega_0}{c} z \frac{dI(t)}{dt} \tag{2.31}$$

Now we have added extra frequency terms in the phase of the E-field giving

$$E(t) = E_0 \exp\left(\imath(\omega_0 t - k_0 z - \frac{n_2\omega_0}{c} z I(t))\right) \tag{2.32}$$

The nonlinearity introduces new frequency components which allow for shorter pulse durations than that of the pulse beforehand. However, the phase

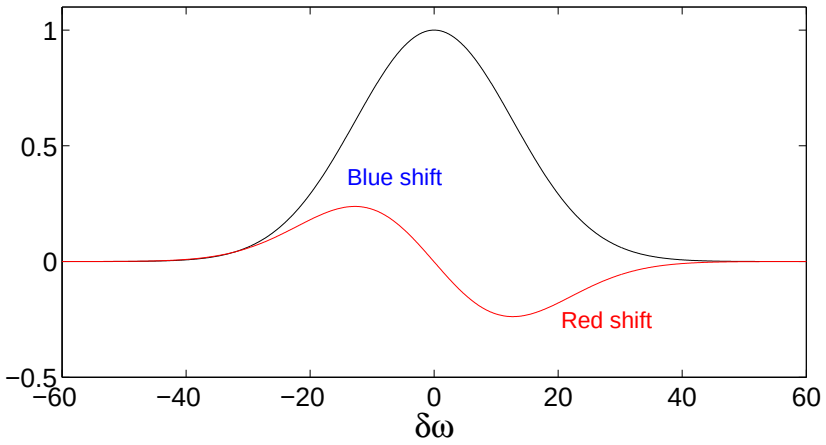

Figure 2.2 Self phase modulation on a gaussian pulse. The gaussian shape is the input pulse. The figure illustrates that as the pulse is rising the is a frequency shift to the blue, while the frequency shift to the red comes from the falling edge of the pulse

of these new frequency components needs to be adjusted before the minimum pulse duration can be attained. This is illustrated in figure... 2.2. This is the principle that the whole theory is based on.

2.3 What is GVD and how do we compensate?

GVD stands for Group Velocity Dispersion which is the pulse duration of light spreading in time as the light propagates through a medium. This is a direct effect of different frequency components in the pulse traveling different

velocities while propagating through a dispersive medium.

The spectral phase of the pulse $\varphi(\omega)$ is nice to deal with because it allows one to just add the phase acquired from the different optical components as the pulse propagates to calculate the total optical phase. We can write $\varphi(\omega)$ as a Taylor expansion around a central frequency ω_0 as

$$\varphi(\omega) = \sum \frac{1}{n!}\varphi^{(n)}(\omega_0)(\omega - \omega_0)^n \tag{2.33}$$

which to a second order expansion is

$$\varphi(\omega) = \varphi(\omega_0) + \varphi'(\omega_0)(\omega - \omega_0) + \frac{1}{2}\varphi"(\omega_0)(\omega - \omega_0)^2 + ... \tag{2.34}$$

The second derivative term $\varphi"(\omega_0)$ is the only one to have an effect on pulse shape, if the higher order terms are negligible. We can ignore these higher order terms because the material dispersion far from resonances can be described in terms of a Taylor expansion. Thus our GVD is

$$GVD = \frac{1}{2}\varphi"(\omega_0)(\omega - \omega_0)^2 \tag{2.35}$$

2.3.1 Some sources of GVD

The dispersion parameter for a uniform medium is defined as

$$D = -\frac{\lambda}{c}(\frac{d^2n}{d\lambda^2}) \tag{2.36}$$

$$\varphi(\omega) = \frac{\omega}{c}n(\omega)D \tag{2.37}$$

If $D \geq 0$ then the medium is said to be anomalously dispersive and add negative GVD. The pulse becomes negatively chirped. On the other hand if $D \leq 0$ the medium adds positive GVD, thus applying a positive chirp on the pulse. Most media a pulse travels through has positive dispersion. This is because we are typically below the resonance frequencies of most optically transparent materials.

Specialized optics/optical systems need to be developed to provide a negative chirp if one has an excess of positive GVD from various media and non-linear optical phenomena. See figure 2.3 for a chirped gaussian pulse

To get the shortest pulse possible precompensation is a method typically done with the compressor in the amplifier to try to get rid of any GVD the pulse may see from lenses and other materials before the filament occurs inside the cell. Unfortunately this method is not useful for GVD that is added from the formation of the filament on, because of the nonlinear optical phase imprinted on the pulse in the cell.

Compression is a technique in which the spectral phase of the pulse that

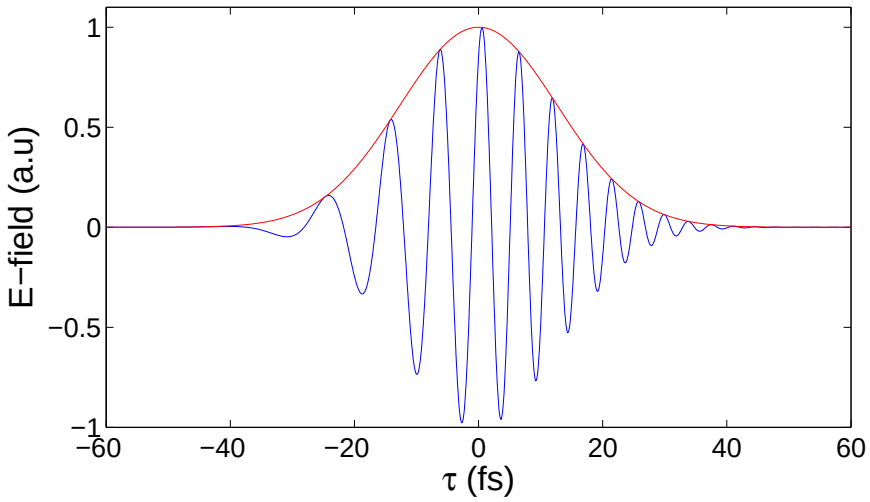

Figure 2.3 E-field of a positive, linearly chirped pulse.

exits the cell is flattened. If the spectral phase is completely flat, then the minimum pulse duration possible is set by the optical spectral bandwidth the pulse carries. This is known as a "transform-limited" pulse. Various methods exist to compress a pulse that are fairly simple to incorporate into ongoing experiments. Two methods commonly used are a grating compressor and a Prism Pair Compressor. These methods however were not chosen to compress the pulse for this project. They were merely mentioned for the realization of other possible pulse compression options.

Chirped mirrors offer yet another possibility for pulse compression and is the method of choice for this project. Chirped mirrors are dielectric mirrors in which the Bragg condition is not constant and varies at different layers with

in the structure. So different frequencies penetrate to different extents and overall see a different group delay. Long wavelengths penetrate deeper into the structure, and thus see a larger delay. The chirped mirrors used here have $50fs^2$ per bounce GVD compensation.

If a system has a total positive GVD, then negative GVD can be provided by chirped mirrors. This method of pulse compression allows for the higher frequency components, which slow in a positively chirped environment, to catch up to the lower frequency components. Therefore minimizing the overall temporal spreading of the pulse in efforts to create a "transform-limited" pulse.

For a very detailed paper on the theory and design of chirped mirrors see [16].

As one gets into shorter and shorter pulse durations, more and more attention must be given to any possible pulse spreading.

Chapter 3

Instruments

This chapter will cover three main areas. The first will be the design of the vacuum cell, the second being a brief discussion on how to use the cell, and finally other instrumentation involved in the project.

3.1 Cell design

The apparatus built as this project is labeled the "cell". It is simply a long hollow vacuum tube filled with an inert gas, with a low dispersion transparent window on each end to allow the passing of light.

The cell was constructed out of KF-40 vacuum tubing with connections to allow for vacuum pumping, pressure monitoring, and filling it with argon gas.

Initially tests were done with the nitrogen in the air at atmosphere to see the filament and obtain spectra using an CCD coupled spectrometer **??**.

Pulse compression and FROG measurements were not obtained for this data. We were only interested in the spectral broadening associated with air at atmosphere. Data will be discussed in chapter 4.

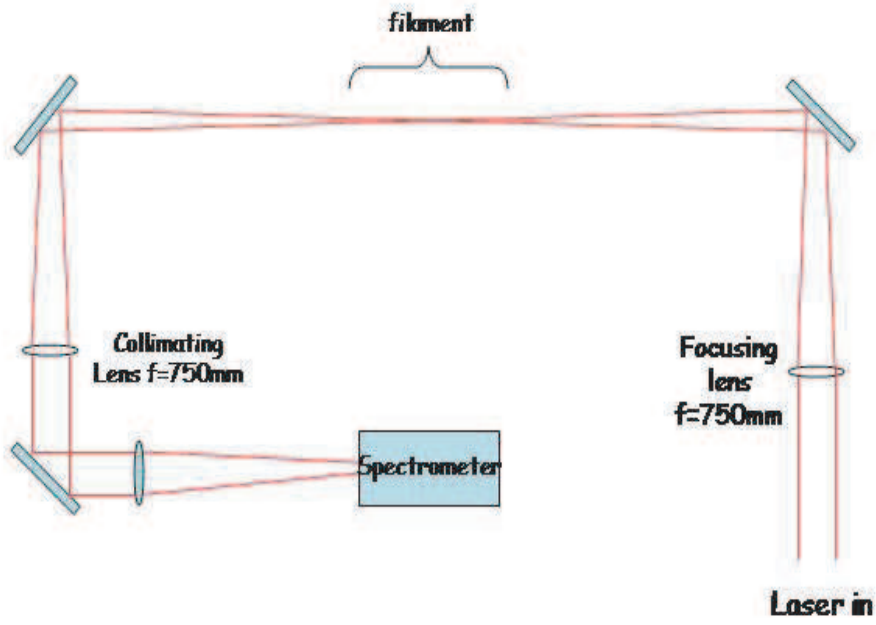

Figure 3.1 design for initial air tests

The project design can be seen in figure .

Special window mounts were machined to be compatible with the KF40 the cell was made of. The entrance window is a Tower Optics fused silica 5mm

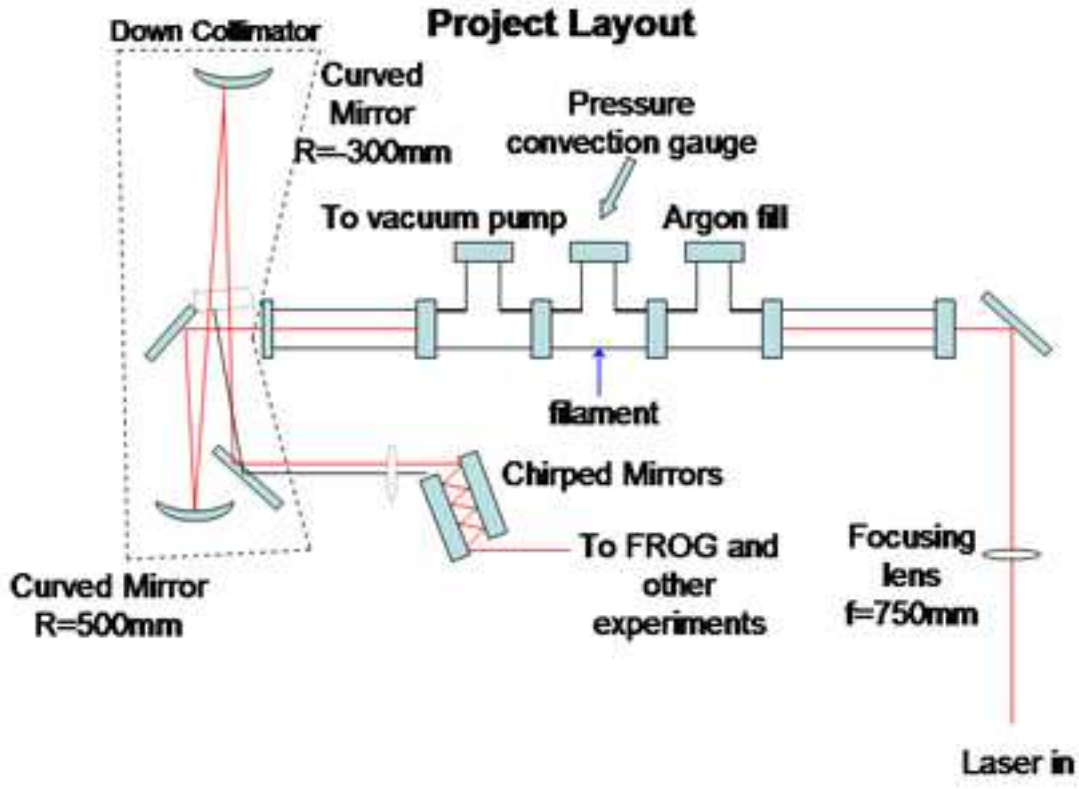

Figure 3.2 The filament forms inside the cell generating more colors. The light is then down collimated with curved optics to decrease the beam spot size. The pulse is compressed through chirped mirrors before propagating to other experiments

thickness, 1inch diameter window. The design of the window can be seen in the following figure.

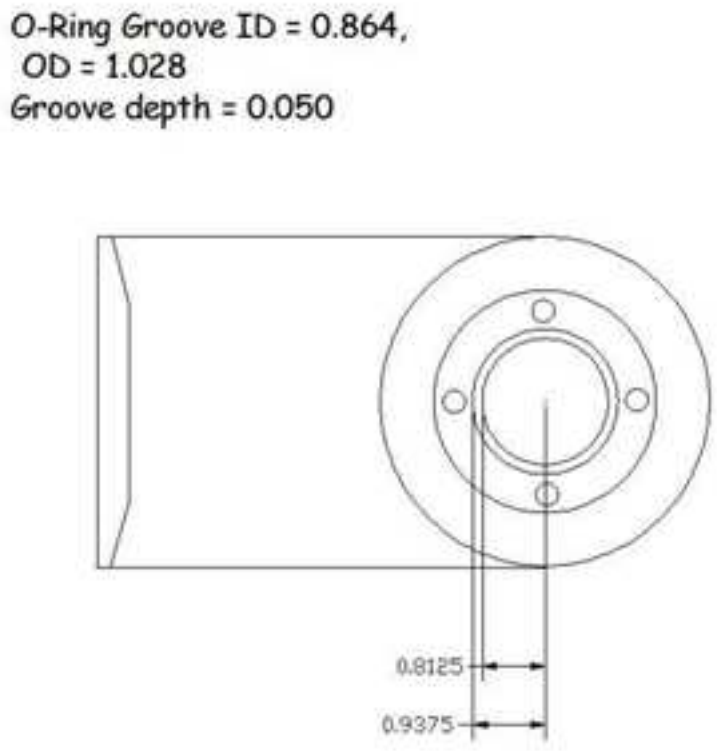

Figure 3.3 Window mount specification produced with AutoCAD 2006

It simply incorporates a 13/16" diameter hole with an o-ring groove centered 1/8" outside the hole. Since the window is 1" in diameter, the center of the material for the o-ring needed to lie no further than 1/16" from the outside edge of the window to provide decent support.

The exit window could not be of the same thickness or material as the entrance window due to the effects of GVD after the filament. We can prec-

ompensate for the material the beam goes through before the filament to produce a transform limited pulse near the filament, giving us maximum spectral bandwidth with the amplifier, but not for what comes after. So some caution needs to be observed about what material we let the beam pass through, and if that material is going to stretch the pulse out considerably or not. The exit window available was a 20mm diameter, $250\mu m$ thick sapphire window glued to another blank KF40 end cap. The sapphire window helps minimize the total GVD on the pulse to make compression easier.

Curved mirrors were used to down collimate the spot size of the beam and not add GVD to the pulse by going through optics. At the exit of the cell the spot size is too large to fit enough bounces on chirped mirrors to provide ample compression of the pulse. We require about four bounces on each chirped mirror, so we had the to down collimate by a factor of almost 3. The beam is still diverging at the exit window, so curved optics were placed in such a position as to focus the diverging beam to a suitable spot size before being collimated. Collimation before down collimation would have been easier to setup and calculate, but would have also provided some power losses from the mirrors. The positions and focal lengths of the required optics were calculated using gaussian beam theory discussed in chapter 2. Table 3.1 is the various curved mirror position parameters with corresponding down

CM 1 (mm)	CM 2 (mm)	DC factor
1400	1656	3.20
1430	1674	2.85
1440	1681	2.80
1460	1696	2.73
1480	1710	2.59
1500	1725	2.50
1600	1803	2.00

Table 3.1 Curved mirrors positions for beam down collimation. The position are distance from the focusing lens prior to the cell. CM1 is the first curved mirror (R=500mm) the beam encounters, while CM2 is the second (R=-300mm).

collimation factors.

The data seen in table 3.1 is the mirror positions, relative to the initial focusing lens, for various spot size down collimation factors. down collimating too much increases the peak intensity of the pulse to a point where various optical elements could become damaged. So we want to down collimate enough to work with a varying number of bounces on chirped mirrors, to find the best pulse compression, and keep any optical elements in the system safe.

3.2 How to use the cell

3.2.1 Alignment

Keeping the beam intensity turned down is the safest way to propagate the beam down to and through the cell. The beam makes several bounces off mirrors and through a periscope, which can be dangerous even with the power turned down. This can be adjusted in the amplifier by turning a wave plate. Making a note of the initial position of the wave plate before making any changes allow's one to easily return to the previous settings.

Proper alignment into the cell is critical in that clipping of the beam can occur very easily on the sapphire exit window. The alignment is performed using two iris'. One of which is approximately 2.5m from the cell, and the other is right at the entrance to the cell. This allows for position and angle alignment forcing the beam to enter straight on and not at some arbitrary angle. Once aligned through the irises, propagation through the cell is allowed. If one achieved good alignment into the cell, then alignment through the down collimator and chirped mirrors afterward should be minimal. Caution is observed as to make sure that the beam is not clipping on any of the optics. This is not only dangerous, but can also result in loss of critical beam intensity and bad data.

3.2.2 Pressurizing with argon

Once the beam is aligned through the cell, and the FROG instrument, then the cell can be pressurized with argon. The procedure for letting argon in is somewhat tricky. If not observed, the cell could pressurize to fast to above atmosphere, and force a leak in the windows. Even worse someone could get hurt if the window happened to be shot off. The cell is NOT to be pressurized above 1atm (760 Torr) for experimentation.

First we pump out the cell to roughing vacuum, approximately 10^{-2} Torr via a mechanical roughing pump out in the hallway. The vacuum valve on the cell is usually open when we are not running an experiment. It should only take 3-5 minutes for the cell to be completely pumped down. Pumping out the argon line is also necessary because it just allows the vacuum to take out as much of the air that may be in the system as possible.

Open the main valve on the argon tank next to the regulator pressurizes the regulator. The black knob on the regulator is the argon gas flow control. Caution is observed here to not pressurize the cell too fast. Typically one can allow the argon to flow right into the cell without keeping the inline gas valve closed, if going up to a few hundred Torr. The convection gauge on the cell used to measure pressure is not calibrated for argon gas but nitrogen. There is a calibration curve just above the tank that converts gauge reading to

actual pressure inside the cell. Repeating this procedure a few times allows a more pure sample of argon to enter the cell for the final fill up to the pressure desired. The back regulator knob is closed once we are done using the argon

Adjusting the pressure once all of the valves are closed is tricky. The simplest way to increase or decrease the pressure is to open the vacuum valve on the cell and let some argon out. It is easier to control the pressure if you have a constant flow through the regulator coming from a lower pressure to a higher pressure. Typically we drop the pressure first then bring it back up to the new pressure, and keep all of the valves closed while running an experiment

3.3 FROG

Frequency Resolved Optical Gating is a technique in which ultrashort pulses can be measured and characterized [17]. The technique is based on Second Harmonic Generation (SHG) using the pulse to measure itself. It tells us phase, τ, spectral bandwidth, and symmetry information about the pulse. Basically the pulse is split in an interferometer, where the pulse from one path is used as a gate, while the pulse from the other path is the probe and are recombined in a nonlinear crystal allowing them to interact with each other with SHG. This means the spectrum recorded on a spectrometer is a "time-slice" of the pulse itself. Figure 3.4 is a layout for a SHG FROG system. For

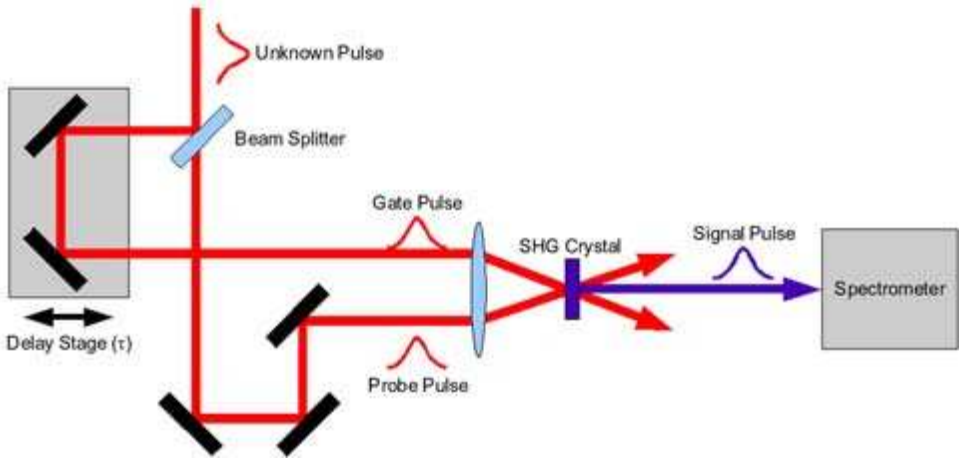

Figure 3.4 SHG Frog layout

my setup, a 100 μm nonlinear crystal is used for SHG. A thicker crystal could be used but then the phase matching conditions are not met and cause some distortion of the pulse. FROG data will be discussed in the next chapter.

Chapter 4

Results, Calculations, and Characterization

There were three different parameters measured when characterizing this device, the pulse duration and phase, spectral bandwidth, and mode quality. These are important measurements because using a pulse with unknown parameters is not practical. The aim here is to see what conditions must be met to yield the shortest pulse and to see how sensitively the pulse duration depends upon argon pressure and peak laser intensity.

The expectation is that we should be able to find some minimum τ as a function of varying argon pressure and pulse energy. At very low pressure we should have no SPM, while a high energies we will get some ionization of the gas forming a plasma that can affect the mode both spatially and temporally. τ should decrease with increasing pressure up to an atmosphere. SPM should scale roughly linearly with pressure.

4.1 Measurements and results

4.1.1 Spectra

One of the everyday tasks when one routinely brings up the laser is to record a spectrum out of the amplifier. This lets us know what kind of bandwidth we have for experimentation. We measure the spectrum by directing a small portion of the beam into a CCD coupled spectrometer. It is often enough, for a quick measurement, to take the diffuse light that reflects off of a white card. The spectrum is used for comparison with cell spectra to see the broadening difference, as well as a rough measure as to what the shortes possible τ is for that day. Using a simple LabVIEW program, we can calculate the shortest possible pulse duration for a given bandwidth. Typically one uses the compressor adjustment in the amplifier to produce the shortest pulse, and so τ for the spectrum to pulse calculation on the given spectrum is very close to the real τ that we measure. The actual pulse duration is measured for the amplifier using the FROG technique discussed in chapter 3 with measurements discussed in section 4.1.2. A typical spectrum can be seen in figure 4.1 which has about 35nm FWHM of bandwidth and returns a pulse duration of about 28fs. The spectrum has some noise fluctuations in it, which is mainly due to speckle of of the white card. Since the card is not a mirror its surface has inconsistencies

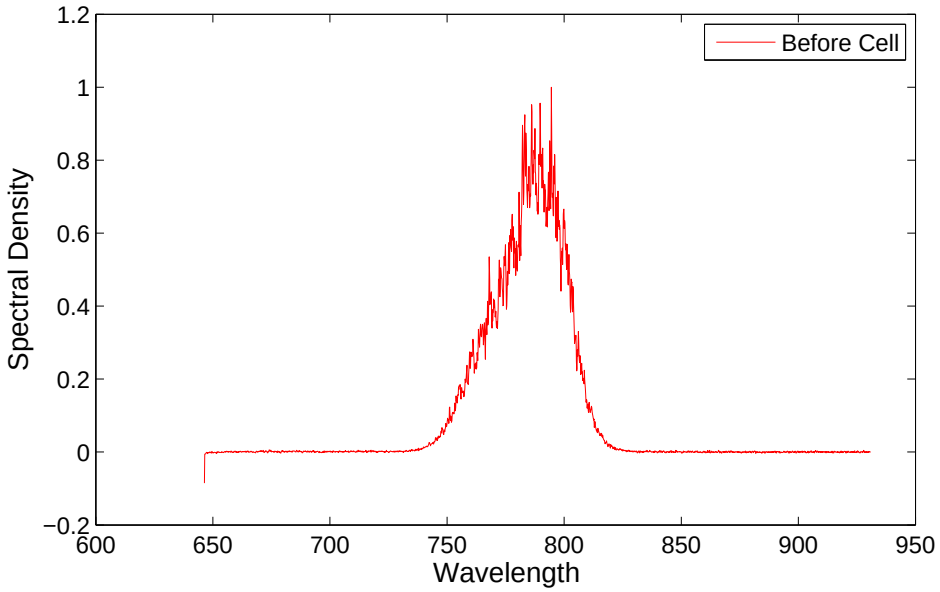

Figure 4.1 Amplifier Spectrum

that cause constructive and destructive interference thus causing the fuzziness in the amplifier spectrum. Focusing directly into the spectrometer would eliminate this. This noise is not real, in the sense that it is not from the laser, so it is not of great concern. The laser, however, does have some intrinsic noise that can be characterized by histograms that illustrate how much noise one has in their system. This noise could have a negative impact on the spectrum that would exit the cell. The laser noise arises from some fluctuations, in current and temperature, in the pump laser for the oscillator and from instability in the mounts in the oscillator. Since we have an output signal that relies on a nonlinear process to obtain the desired results, this noise tends to become

amplified. At this point histograms have not been made for the exit beam of my cell. However, they are a significant part of the characterization process.

Since the spectrum bandwidth to pulse duration calculation is a not an actual τ measurement, we can measure the τ we have using FROG. FROG allows us to completely characterize the ultrashort pulse from the cell in time from pulse duration to reconstructing the E-field and phase. The FROG reconstruction temporal FWHM, for figure 4.1, $\tau = 29$fs. This shows that the actual τ is very close to the shortest possible τ, given the spectral bandwidth we have.

The spectrum seen exiting the cell is substantially broadened with respect to the amplifier spectrum. This is exactly what we were looking for, because this broadened spectrum in principle allows to generate a shorter pulse. This spectrum was acquired using a the maximum pulse energy attainable at the entrance to the cell ($900\mu J$) and an argon gas pressure of 660 Torr. Argon is ideal because argon has a high ionization potential, which means the generation of pulse distorting ions is minimal. This is beneficial because the dispersion of a plasma can be strong depending on the density. Figure 4.2 shows the broadened spectrum compared to the amplifier spectrum. One can easily see that self phase modulation inside the cell causes dramatic broadening of the spectrum.

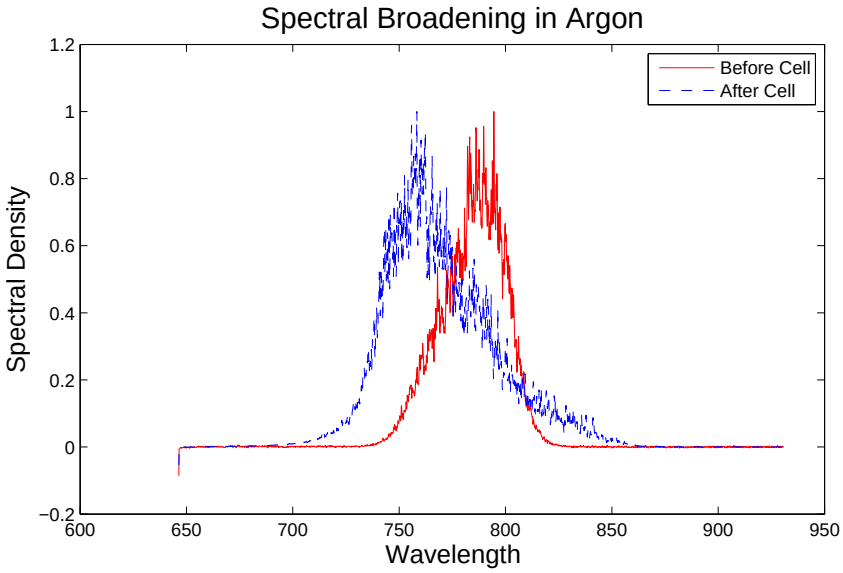

Figure 4.2 Broadened spectrum with a pulse intensity of $900\mu J$ and argon pressure of 660 Torr

With the input bandwidth of about 35nm we obtain a broadened bandwidth of roughly 83nm. The actual bandwidth achieved from the broadening in the cell is dependent upon pulse energy and argon gas pressure, both discussed below in section 4.1.2, as well as the position of the compressor in the amplifier. Before, we adjusted the compressor in the amplifier to achieve the shortest pulse possible. Now we want to adjust the compressor to maximize the bandwidth that exits the cell. This in principle precompensates for any GVD the pulse obtains before the formation of a filament, and places a "transform-limited" pulse somewhere in the filament, providing as broad of a

bandwidth at the output of the cell as possible. The shortest τ possible from the broadened spectrum is $\tau = 19.3fs$. The next step is to see what is required to actually attain a pulse this short.

4.1.2 Pressure and intensity dependencies

Cell pressure and pulse intensity play an extremely important role in output pulse duration. This section will map out how the pressure and intensity affect the transformation of the pulse.

First, the beam that exits the cell has a large amount of GVD that is spreading the pulse duration of 19fs out to $\simeq$ 180fs. This requires compression from the chirped mirrors discussed in Chapter 3. To compensate for this GVD we used two chirped mirrors with four bounces per mirror.

The mode of the beam at roughing vacuum ($\simeq 10^{-2}$ Torr) is very close to gaussian.

The spot sizes of the modes in figure 4.3 are roughly 1.7 mm at the 1/e point of the field. This suggests that the mode spot size does not change with increasing pulse energy and pressure.

After the SPM occurs the beam makes its way out of the cell. We were concerned about the fact that too high of a pulse energy, would form a plasma and cause diffraction of the light inside the filament, thus changing the shape of

the mode. The mode itself didn't change, but we now have a very pronounced ring around the mode. See figure 4.4 below.

Pulse measurements were made using a FROG and reconstructed with Femtosoft FROG software. The SHG blue light demonstrated in figure 3.4 was maximized by adjusting the temporal overlap with a mirror on the non-moving arm. The reconstructions return temporal, spectral, and phase information about the the pulses. Figure 4.5 are frog reconstructions for $I = 800\mu J$ and pressure $P = 720$ Torr.

We have obtained a pulse duration of $\tau \simeq 19.3fs$ with a spectral bandwidth of approximately 71nm after compression.

Pulse measurements were made with FROG by taking six energies at the entrance of the cell from $500\mu J - 950\mu J$ and varying the pressure from 100 Torr - 720 Torr. The intention here was to create a plot to locate the best possible pressure and energy combination that returns the shortest pulse without distorting the mode.

First, plots of pulse duration vs. pressure, and pulse duration vs. pulse energy were created and can be seen in figures 4.6 and 4.7 respectively.

Figure 4.6 shows a decline in τ for an increase in pressure. This suggest that we should find the shortest pulses at high pressures. The dependence on pulse energy in the range from 500 to 950 μJ is rather weak, and this is quite

beneficial to us because it means that we will be able achieve relatively short pulses for a large range of pulse energies. Over a range of $450\mu J$, τ overall only changes $2-3fs$. This is not a substantial difference in comparison with how τ depends on argon pressure. The data also suggests that maximizing the pulse energy is not desirable. This means that if we want to use high energies we should consider changing the focal geometry by using a longer focal length lens. This would create a more stable mode, decrease the peak intensity of the beam (allowing for the high pulse energies), provide frequency broadening without creating a plasma, and retain the short τ.

Now with figures 4.7 and 4.6 we can construct a surface plot which shows the dependence of the output pulse duration on pressure and pulse energy. See figure 4.8.

The graph shows that a minimum seems to exist at low pressures and pulse energies. Our expectation was that we would find some minimum τ for varying pressure and energy, and we did. However, for the experiments conducted in the lab, we need higher pulse energies ($\sim 800-900\mu J$) than the $500\mu J$ that gives us the shortest τ. The best pressure/pulse energy combination for us is approximately at 720 Torr and 800 μJ, giving us a compressed τ of 19.3 fs.

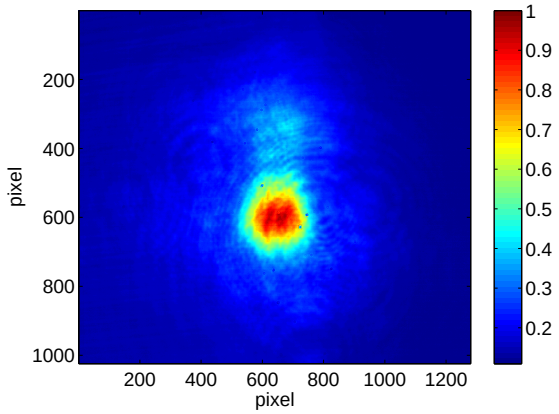

(a) a.

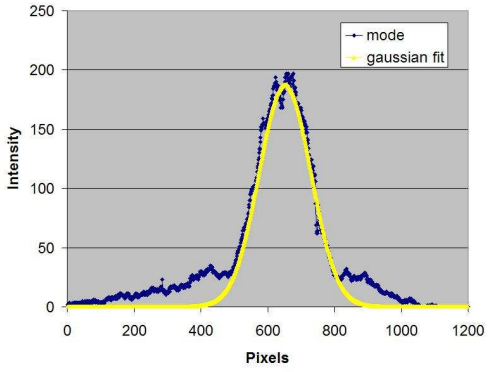

(b) b.

Figure 4.3 (a) is the mode of the beam. There is a back reflection off of a ND filter that can be seen just above the main spot, and (b) is the beam profile in a vacuum. It has been background subtracted and fit with a gaussian. This is a line out in the horizontal direction of (a).

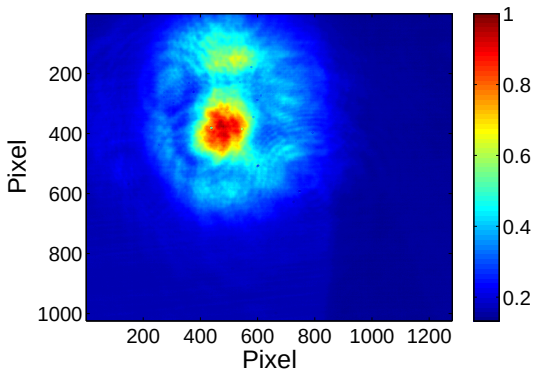

(a)

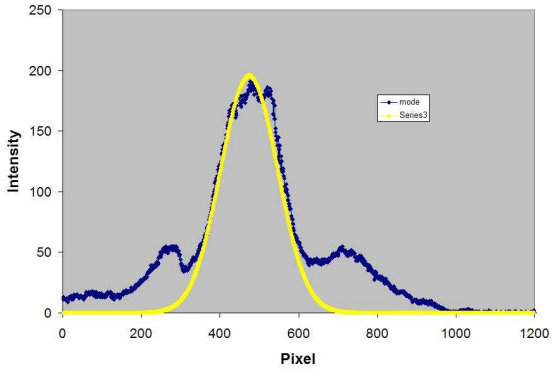

(b)

Figure 4.4 The figure illustrates the shape of the beam mode after passing through the cell. In (a) the mode itself is slightly distorted with an obvious ring around the mode. (b) shows the horizontal cut creating a beam profile.

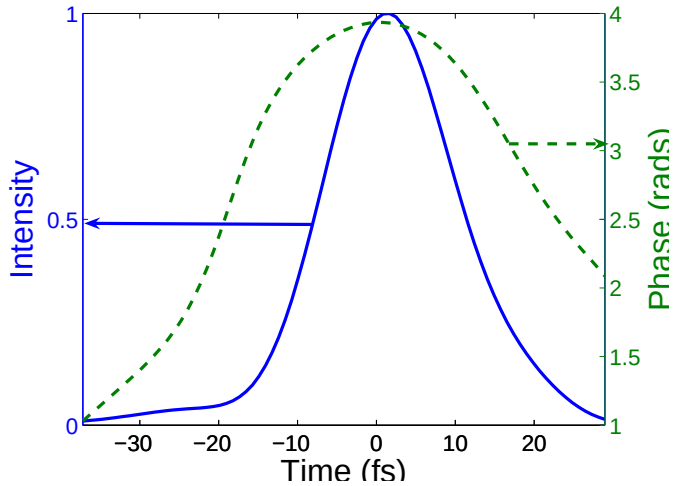

(a)

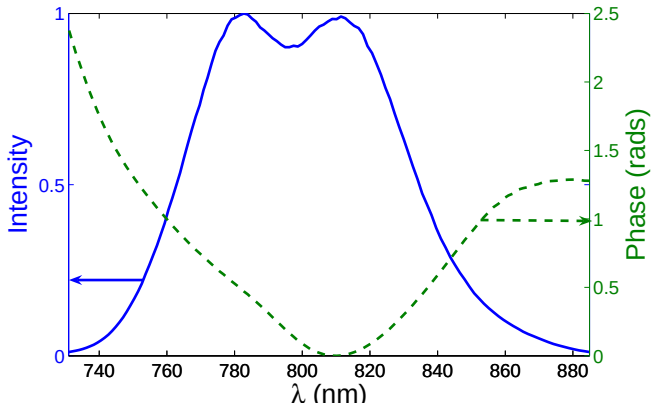

(b)

Figure 4.5 We can see in (a) the temporal reconstruction of the pulse while (b) shows us the spectral reconstruction. These plots show phase on the right hand side and relative intensity on the left

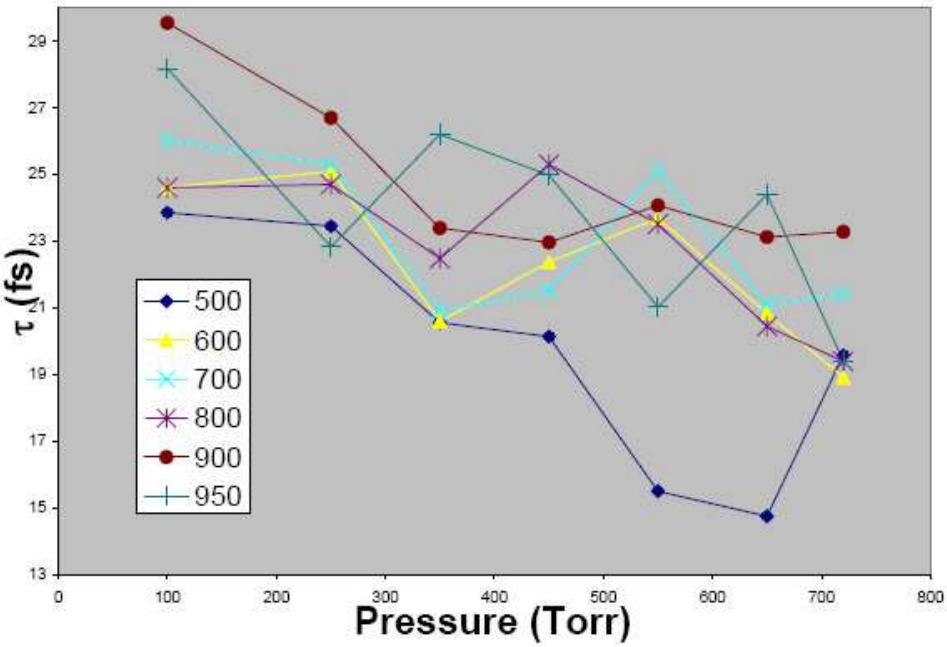

Figure 4.6 Pulse duration vs. Cell pressure. The legend is for different intensities and is in μJ.

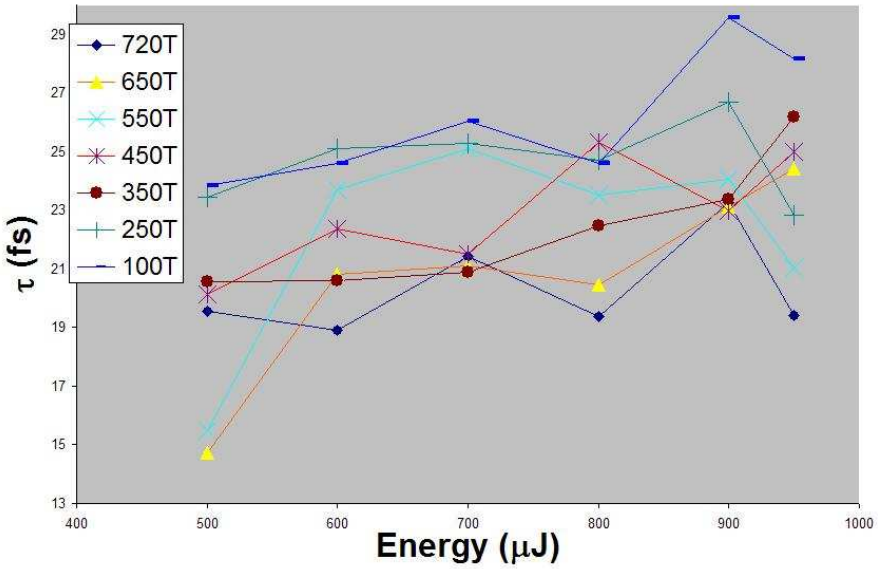

Figure 4.7 Pulse duration vs. Intensity for different pressures.

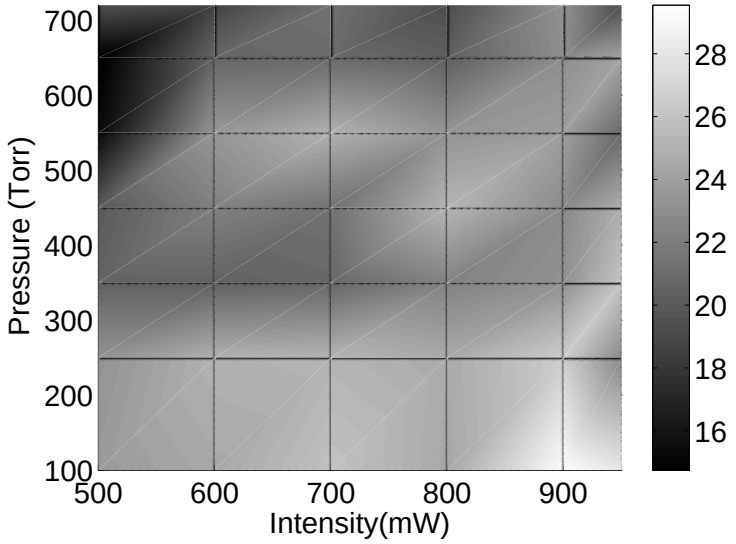

(a)

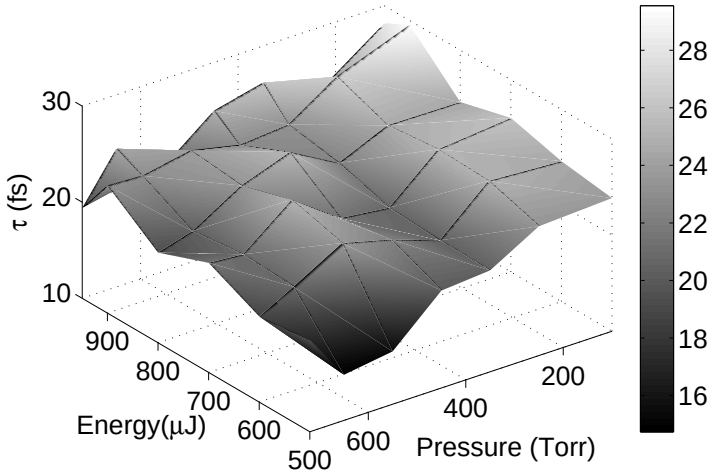

(b)

Figure 4.8 (a) is a surface plot of τ with the colorbar on the right showing the τ scale and (b) is the 3D version to show a slope and a minimum

Chapter 5

Conclusions and Future Work

In conclusion we were successful in the design and construction of a system to produce broad bandwidth, high energy, and reasonably flat phase sub-20 fs pulses that is far more inexpensive and much easier to build and maintain than the hollow core fiber setup. We have consistently achieved pulses with a compressed τ as short as 19 fs with a spectral bandwidth of 70 nm, and have observed the pressure and pulse energy dependencies on these short pulses through detailed characterization of this setup. Experiments with the pulses from this system were not done before the time of this thesis. Through the characteriztion of the system we have confirmed that our requirements have bet met for the pulse parameters. These pulses will be used for ongoing experiments in the area of strong field atomic physics.

Bibliography

[1] W. Sibbett" "D.E. Spence, P.N. Kean. "60-fs pulse generation from a self-mode-locked ti:sapphire laser". *"Optics Letters"*, 16(21):1762, November "1991".

[2] Aquavella J. Zhao Y. Wang, J. and S. Chung. Tear dynamics measured with real-time optical coherence tomography. *Journal of Vision*, 4(11):89a, 2004.

[3] J. Shah. *Ultrafast spectroscopy of semiconductors and semiconductor nanostructures*. Springer-Verlag, Berlin, 1996.

[4] Dan; Silberberg Yaron Polachek, Lea; Oron. Full control of the spectral polarization of ultrashort pulses.

[5] Langchi Zhu, Valeria Kleiman, Xiaonong Li, Shao Ping Lu, Karen Trentelman, and Robert J. Gordon. Ultrafast coherent control and destruction of excitons in quantum wells. *Phys. Rev. Lett.*, 75(13):2598–2601, 1995.

[6] T. Hornung, R. Meier, r. de Vivie-Riedle, and M. Motzkus. Coherent control of the molecular four-wave-mixing response by phase and amplitude shaped pulses. *Chem. Phys.*, 267:261–276, 2001.

[7] Ahmed H. Zewail J. Spencer Baskin. Ultrafast electron diffraction: Oriented molecular structures in space and time. *ChemPhysChem*, 6(11):2261–2276, 2005.

[8] A. Assion, T. Baumert, M. Bergt, T. Brixner, B. Kiefer, V. Seyfried, M. Strehle, and G. Gerber. Control of chemical reactions by feedback-optimized phase-shaped femtosecond laser pulses. *Science*, 282:919–922, 1998.

[9] R. Holzwarth Th. Udem and T. W. Hnsch. Optical frequency metrology. *Nature*, 416:233–237, 2002.

[10] Patrick Henning Nurnberger and Thomas Weinacht. Design and construction of an apparatus for the neutral dissociation and ionization of molecules in an intense laser field. Master's thesis, Stony Brook University, 2003.

[11] P. Maine "J.S. Coe and P. Bado". "regenerative amplification of picosecond pulses in nd:ylf: gain narrowing and gain saturation". *"Journal of the Optical Society of America B"*, 5(12):2560–, December "1988".

[12] S. De Silvestri M. Nisoli and O. Svelto. Generation of high energy 10 fs pulse by a new pulse compression technique. *Applied Physics Letters*, 68(20):2793–2795, March 1996.

[13] F.W. Helbing A. Heinrich A. Couairon A. Mysyrowicz J. Biegert U. Keller C.P. Hauri, W. Kornelis. Generation of intense, carrier-envelope phase-locked few-cycle laser pulses through filamentation. *Applied Physics B: Lasers and Optics*, 79:673–677, 2004.

[14] "Peter W. Milonni and Joseph H. Eberly". *"LASERS"*. "John Wiley and Sons", "1988".

[15] Anthony E. Siegman. *Lasers*. University Science Books, Sausalito, 1986.

[16] "R. Szipocs and A. Kohzi-Kis". "theory and design of chirped dielectric laser mirrors". *"Applied Physics B: Lasers and Optics"*, 65(2):115–135, August "1997".

[17] Rick Trebino, Kenneth W. DeLong, David N. Fittinghoff, John N. Sweetser, Marco A. Krumbugel, Bruce A. Richman, and Daniel J. Kane. Measuring ultrashort laser pulses in the time-frequency domain using frequency-resolved optical gating. *Rev. Sci. Instrum.*, 68(9):3277–3295, 1997.